Published in final edited form as:
J Invest Dermatol. 2010 June ; 130(6): 1726–1736. doi:10.1038/jid.2009.362.

Molecular Analysis of Tumor-Promoting CD8+ T Cells in Two-Stage Cutaneous Chemical Carcinogenesis

Bernice Y. Kwong[1], **Scott J. Roberts**[1], **Tobias Silberzahn**[2], **Renata B. Filler**[1], **Jason H. Neustadter**[1], **Anjela Galan**[1], **Swapna Reddy**[1], **William M. Lin**[1], **Peter D. Ellis**[3], **Cordelia F. Langford**[3], **Adrian C. Hayday**[2,4], and **Michael Girardi**[1]

[1] Department of Dermatology and Skin Diseases Research Center, Yale University School of Medicine, New Haven, Connecticut, USA

[2] Peter Gorer Department of Immunobiology, King's College London School of Medicine at Guy's Hospital, London, UK

[3] The Wellcome Trust Sanger Institute, Wellcome Trust Genome Campus, Hinxton, Cambridge, UK

[4] London Research Institute, Cancer Research UK, London, UK

Abstract

T-pro are tumor-infiltrating TCRαβ$^+$CD8$^+$ cells of reduced cytotoxic potential that promote experimental two-stage chemical cutaneous carcinogenesis. Toward understanding their mechanism of action, this study uses whole-genome expression analysis to compare T-pro with systemic CD8$^+$ T cells from multiple groups of tumor-bearing mice. T-pro show an overt T helper 17–like profile (high retinoic acid–related orphan receptor-(ROR)γt, IL-17A, IL-17F; low T-bet and eomesodermin), regulatory potential (high FoxP3, IL-10, Tim-3), and transcripts encoding epithelial growth factors (amphiregulin, Gro-1, Gro-2). Tricolor flow cytometry subsequently confirmed the presence of TCRβ$^+$ CD8$^+$ IL-17$^+$ T cells among tumor-infiltrating lymphocytes (TILs). Moreover, a time-course analysis of independent TIL isolates from papillomas versus carcinomas exposed a clear association of the "T-pro phenotype" with malignant progression. This molecular characterization of T-pro builds a foundation for elucidating the contributions of inflammation to cutaneous carcinogenesis, and may provide useful biomarkers for cancer immunotherapy in which the widely advocated use of tumor-specific CD8$^+$ cytolytic T cells should perhaps accommodate the cells' potential corruption toward the T-pro phenotype. The data are also likely germane to psoriasis, in which the epidermis may be infiltrated by CD8$^+$ IL-17-producing T cells.

INTRODUCTION

The capacity of CD8$^+$ cytolytic T cells (CTLs) to lyse malignant cells showing tumor-associated antigenic peptides on surface major histocompatibility complex-I underpins a major immunotherapeutic emphasis on CD8$^+$ T-cell stimulation (see Finn, 2008). Indeed, several human tumors, including colon and ovarian carcinoma, show an association of

Correspondence: Michael Girardi, Department of Dermatology, Yale University School of Medicine, 333 Cedar Street, HRT 616, New Haven, Connecticut 06520-8059, USA. girardi@yale.edu.

Sites of experiments: New Haven, Connecticut, USA; London and Hinxton, UK

CONFLICT OF INTEREST

The authors state no conflict of interest.

improved prognosis with the degree of $CD8^+$ tumor-infiltrating lymphocyte (TIL) (Galon *et al*., 2006; Tomsová *et al*., 2008). However, tumor-specific CTL-based immunotherapy has met with limited success, an outcome attributed to several opposing immunologic forces, including $CD4^+$ T-regulatory (T-reg) cells, tumor-associated macrophages (TAM) (Allavena *et al*., 2008), and other systemic and local immunosuppressive mechanisms (Quezada *et al*., 2008); and the concomitant stimulation of tissue hyperproliferation and oxidative reactive species fostered by inflammatory cells (Coussens and Werb, 2002). Nonetheless, little attention has been paid to the potential of $CD8^+$ T cells themselves to enhance tumor growth.

Using a well-established two-stage model of chemical carcinogenesis, which provokes the development of cutaneous papillomas followed by variable progression to squamous cell carcinomas (Hennings *et al*., 1981), we earlier identified a previously unknown $TCR\alpha\beta^+CD8^+$ tumor-promoting T-cell (T-pro) subset that has reduced cytolytic potential and substantially enhances carcinogenesis (Roberts *et al*., 2007). T-pro compose the first $CD8^+$ T-cell subset specifically associated with tumor promotion, joining $CD4^+$ T-reg as a focus of biological and clinical interest in the immunopathogenesis of cancer progression.

The functional phenotypes of several T-cell subsets are largely dependent on the distinctive activities of several transcription factors, for example, T-bet, transcription factor GATA binding protein-3 (GATA-3), FoxP3, and retinoic acid–related orphan receptor-(ROR)γt that promote the differentiation of $CD4^+$ T cells into T helper (TH)1, TH2, T-reg, and TH17 cells, respectively. Several investigators have suggested that TH17 cells might be further subdivided into “effector TH17” cells that primarily produce IL-17, and “regulatory TH17” cells that also express FoxP3 and produce the immunosuppressive cytokine, IL-10 (Lochner *et al*., 2008; McGeachy and Cua, 2008). As the TH1 and TH17 pathways may both be proinflammatory, and because epidemiological data clearly identify inflammation as a predisposing factor for carcinogenesis (Swann *et al*., 2008), we hypothesized that T-pro may represent a $CD8^+$ counterpart of a TH1 or a TH17 response. In this regard, it was recently shown that T-bet directs $CD8^+$ T-cell differentiation into perforin-producing CTLs only when there is concomitant expression of high levels of the related transcription factor eomesodermin (Eomes) (Intlekofer *et al*., 2008). This joint requirement for T-bet and Eomes was elucidated during lymphocytic choriomeningitis virus challenge in which instead of providing cytolytic responses, $CD8^+$ T cells deficient in both factors adopted an alternative, proinflammatory phenotype with striking similarities to $CD4^+$ TH17 cells. Recently, $CD8^+$ IL-17-producing T cells have been identified in additional contexts, including psoriasis (Kryczek *et al*., 2006) and in several experimental and human tumors (Kryczek *et al*., 2007). Thus, it is possible that the milieu of skin inflammation and/or malignancy may dramatically influence $CD8^+$ T-cell differentiation and effector function away from cytotoxicity and toward TH17-like properties.

To test whether the reduced cytolytic potential of $CD8^+$ T-pro is associated with a TH17-like phenotype, we subjected the cells to whole-genome expression analyses, quantitative reverse transcriptase-PCR, and flow cytometry. The results show that relative to systemic $CD8^+$ T cells, T-pro are substantially enriched in signatures of regulatory TH17 cells, associated with which they show deficient expression of both T-bet and Eomes. Moreover, T-pro express several epidermal growth factors, including amphiregulin. In addition to providing insight into T-pro cells, the expression profile identified a marker panel for the development of the T-pro phenotype, which we show to correlate with tumor progression. Such may similarly serve as a biomarker for the potential phenotypic corruption of $CD8^+$ CTLs administered in immunotherapeutic regimens.

RESULTS

Carcinogen dose effects on CD8$^+$ T-pro

Previous application of two-stage chemical carcinogenesis at different doses to relevant gene knockout mice, coupled with adoptive transfer studies, has collectively shown that TCR$\gamma\delta^+$ cells predominantly oppose tumor initiation, whereas the effects of the TCR$\alpha\beta^+$ T-cell compartment are mixed: CD4$^+$ $\alpha\beta^+$ cells harbor an immunoprotective component, whereas CD8$^+$ $\alpha\beta^+$ cells include T-pro (Girardi *et al*., 2001; Roberts *et al*., 2007; Strid *et al*., 2008). To determine whether the effects of CD8$^+$ T-pro increase with carcinogen exposure, we compared tumor growth under both low-dose and high-dose 7,12-dimethylbenz[*a*]anthracene (DMBA)/12-*O*-tetradecanoylphorbol 13-acetate(TPA) protocols in wild-type (wt) and CD4$^{-/-}$ mice (that each harbor CD8$^+$TCR$\alpha\beta^+$ cells) and in TCR$\beta^{-/-}$ mice (that do not harbor CD8$^+$TCR$\alpha\beta^+$ cells). At low dose, CD4$^{-/-}$ mice showed significantly higher tumor susceptibility than did wt mice (Figure 1a and b), consistent with the absence of tumor-inhibitory CD4$^+$ T cells from these mice (Girardi *et al*., 2003). However, the reduced tumorigenesis in the TCR$\beta^{-/-}$ strain emphasizes the tumor-promoting effects of $\alpha\beta$ T cells that were previously attributed to CD8$^+$ T-pro by selective knockouts and adoptive transfers (Roberts *et al*., 2007). Conversely, at 15 weeks post initiation with DMBA, wt and CD4$^{-/-}$ strains subjected to high-dose protocols both displayed comparable tumor burdens, >3-fold greater than TCR$\beta^{-/-}$ mice (P<0.001) (Figure 1c–e). Thus, as carcinogen exposure increases, the CD8$^+$ T-pro effect is maximized relative to any protective effects of CD4$^+$ T cells. Consistent with this, CD8$^+$ TILs were substantially enriched in the tumor relative to the stroma (Figure 1f). Therefore, we used this system as a source of T-pro cells to gain insight into their potential mechanism of action.

Gene-expression profiles of T-pro

Highly purified (>98%) CD44^{HI}CD62L^{LO}TCRβ^+CD8$^+$ T-cell populations from TIL and the counterpart peripheral blood lymphocytes (PBLs) of tumor-bearing (Tum$^+$) CD4$^{-/-}$ and wt mice, respectively, were obtained by flow cytometric sorting, and assessed for their expression of ~47,000 genes by use of Illumina Sentrix bead chips (Illumina, San Diego, CA). Absolute probe hybridization values were consistent with high-fidelity purifications; for example, there was no expression of either CD4 or of signature genes for other skin populations, notably Langerhans cells and keratinocytes (Figure 2a). Hierarchical gene-clustering analysis showed striking concordance between the two TIL populations and between the two PBL populations. Moreover, the latter pair was distinct from the TIL and much more similar to phenotypically equivalent, CD44^{HI}CD62L^{LO}TCRβ^+CD8$^+$ effector T cells purified from the PBL of naive animals (that is, those that were not exposed to chemical carcinogens) (Figure 2b). More specifically, of ~800 (~1.7%) genes that were >10-fold differentially expressed by the populations sorted from tumor-bearing mice, relative to CD8$^+$ PBL from naive mice, 724 genes were highly expressed by the CD8$^+$ TIL, compared with only 25 genes enriched in CD8$^+$ PBL from Tum$^+$ mice. These data indicate that the genes underpinning the distinct behavior of CD8$^+$ T cells in Tum$^+$ mice are to be found in the local tumor site rather than in the peripheral compartment.

Among the genes >10-fold upregulated in TIL was RORγt, whereas T-bet and Eomes were between 10- and 100-fold underrepresented in the TIL (Figure 2c). These data predict a TH17-like differentiation pattern and a suppression of cytolytic differentiation, consistent with which IL-17A and IL-17F were within the top 10 most differentially expressed genes in TIL (Table 1; Figure 2c). In addition, there was strong upregulation of IL-6 and IL-23R, both of which contribute to TH17 differentiation (Langrish *et al*., 2005; Langowski *et al*., 2007). The reduced expression of IL-6R suggests these cells may have been previously exposed to IL-6.

Moreover, perforin was among the least represented transcripts in $CD8^+$ TIL, as were RNAs for CTL markers, such as NKG7. TILs were also enriched in transcripts for Foxp3 and IL-10, consistent with T-reg and/or regulatory TH17 differentiation, as well as in transcripts for several other factors that may regulate effector T cells, including IL-4-induced gene 1 (IL4i1) and T cell Ig mucin 3 (Tim-3). Furthermore, the analysis showed a substantial enrichment in TIL of RNAs encoding epithelial growth factors, amphiregulin, Gro-1, and Gro-2. Quantitative reverse transcriptase-PCR (qRT-PCR) analysis of independently sorted populations of $CD8^+$ TIL and PBL isolated from Tum^+ wt and $CD4^{-/-}$ mice fully validated the Illumina data sets (Figure 3).

TH17-like differentiation of $CD8^+$ T-pro

The prediction by gene profiling that $CD8^+$ T-pro resemble TH17 cells was further investigated by the isolation of $TCR\beta^+$ TIL and by the analysis of IL-17 expression in five independent experiments. By contrast to $CD8^+$ PBL from either Tum^+ or naive mice, $CD8^+$ TIL produced IL-17A after TCR stimulation (Figure 4a). Furthermore, the production of IL-17 protein was shown by a substantially greater fraction of $CD8^+$ TIL, by comparison with CD4+ TIL (Figure 4c). However, despite the high transcription expression levels of RORγt and IL-17A, only a minority of the CD8+ TIL produced IL-17 (mean 6.80%; $n = 5$), whereas the same stimulation protocol can produce substantially higher percentages and fluorescent intensities in other TH17-differentiated populations (Ribot *et al*., 2009). Nonetheless, our findings are highly consistent with other systems that have shown biologically relevant IL17-producing CD8+ T cells to compose only a minority of the $CD8^+$ compartment (Hamada *et al*., 2009; Kondo *et al*., 2009).

T-pro profile association with malignant progression

The elucidation of a “T-pro profile” permitted us to track the appearance of T-pro cells. Thus, we examined the expression of the signature genes in $CD8^+$ TIL isolated from malignant carcinomas at 16 weeks after DMBA initiation, in $CD8^+$ TIL isolated at 16 weeks from benign papillomas, and in TIL from week 12 tumors that are smaller and predominantly papillomas. The “T-pro profile” was strongly associated with the $CD8^+$ TIL of malignant tumors (red) than of benign tumors (blue) (Figure 5). Almost all of the previously identified differentially expressed genes found in $CD8^+$ TIL relative to PBL using pooled samples (Figures 2 and 3) were attributable to TIL present within more advanced carcinomas (Table 2), whereas only Tim-3 (upregulated) and perforin (downregulated) were found to be differentially expressed in the TIL of benign papillomas. This suggests a panel of potential biomarkers present within the TIL and specific for malignant progression.

DISCUSSION

Under high doses of DMBA/TPA, the $\alpha\beta^+$ $CD8^+$ T-cell compartment appears to be heavily weighted toward tumor promotion (Roberts *et al*., 2007), and has offered an opportunity to gain a previously unidentified insight into how these cells might facilitate tumor progression, effectively shifting the immune balance during the critical equilibrium state (Koebel *et al*., 2007). The capacity of $CD8^+$ T-pro to locally enhance malignant progression through several major mechanisms is elucidated: fostering a proinflammatory tumor microenvironment, providing specific regulatory activities, and stimulating epithelial cell proliferation. These data indicate that the identified $CD8^+$ T-pro transcripts have immunopathogenic relevance not only to neoplastic growth but specifically also to the progression to carcinoma. As such, these experiments add weight to the idea that the full list of differentially expressed genes will contain other contributors to malignant transformation, and/or T-cell effector functions imparted by the tumor microenvironment. Thus, these genes

can serve as a resource for mechanistic studies, and offer potential targets for cancer prevention and therapy, as well as markers of tumor development and immunotherapy monitoring.

The comparison of our $CD8^+$ T-pro with perforin-deficient $CD8^+$ T cells that have been identified in various other settings offers several parallels, yet also provides major distinctions that suggest that $CD8^+$ T-pro may be unique. Expression analysis of $CD8^+$ T cells chronically stimulated by lymphocytic choriomeningitis virus *in vivo* has shown an "exhaustion" typified by low cytolytic and increased regulatory potential (Wherry *et al*., 2007) that somewhat resembles $CD8^+$ T-pro. Given the important associations between chronic viral infections and malignant transformation, the possibility that $CD8^+$ T-pro are manifested as a direct result of chronic stimulation/exhaustion is an intriguing idea, supported by the relatively lower levels of CD28 and natural killer group 2D transcripts in $CD8^+$ T-pro. However, lymphocytic choriomeningitis virus exhausted $CD8^+$ T cells, relative to their effector precursors, show higher expression of Eomes and FasL, and little IL-17, in large measure, distinguishing these cells from $CD8^+$ T-pro. Liu *et al*. (2007) reported that, under the influence of transforming growth factor-β (TGF-β) and IL-6, $CD8^+$ T cells from naive mixed lymphocyte cultures show downregulation of T-bet and upregulation of RORγt transcription factors. These cells produced IL-17 and showed decreased cytolytic factors. In addition, Hamada *et al*. (2009) used TGF-β, IL-6, IL-21, antibodies to IFNγ, and specific peptide-loaded antigen-presenting cells to generate *in vitro* IL-17-producing $CD8^+$ T cells from TCR transgenic (OT-1) naive $CD8^+$ T cells. These "Tc17" cells were notable for their $CD44^{HI}$ $CD62^{LO}$ phenotype, and showed an expression profile positive for RORγt and FoxP3, and negative for T-bet.

Kryczek *et al*. (2007) found that several human tumors contained $CD8^+$ IL-17-producing cells, and this was echoed in mouse B16 melanoma tumors in which the greatest numbers of such cells were associated with more advanced tumors. These findings, taken together with our present studies of $CD8^+$ TIL versus PBL in tumor-bearing mice suggest that $CD8^+$ T cells recruited from the periphery into the tumor microenvironment are subjected to local factors (for example, produced by the tumor cells or recruited inflammatory cells, such as tumor-associated macrophage) that substantially influence their differentiation and effector function. The downregulation of IL-6Ra observed in our $CD8^+$ TIL specifically suggest that local IL-6 may, through STAT-3 signaling (Harris *et al*., 2007), downregulate T-bet and Eomes and upregulate RORγt in the infiltrating CD8+ T cells. In addition, the downregulation in CD8+ TIL of natural killer group 2D and FasL that we show with tumor progression to malignancy may result from chronic stimulation or soluble ligands released by tumor cells, consistent with our previous findings of immune effects of soluble natural killer group 2D ligands.

Under a "corruption hypothesis" (Figure 6), antitumor $CD8^+$ CTLs may redirect into $CD8^+$ T-pro that inhibit CTLs (for example, through IL-10), enhance chronic inflammation (for example, through IL-17A and IL-17F), and facilitate tumor proliferation (for example, through amphiregulin and Gro-1). Consistent with this, Wakefield and colleagues showed that $CD8^+$ PBL isolated from tumor-bearing mice will produce IL-17A under the *in vitro* influence of TGF-β and IL-6, and revealed that IL-17A itself suppresses tumor cell-line apoptosis by a yet unknown mechanism (Nam *et al*., 2008). Furthermore, several investigators have reported on the potential of IL-17 to directly increase tumor progression, including by its pro-angiogenic effects (Sfanos *et al*., 2008;Zhu *et al*., 2008;Zhang *et al*., 2009). It is possible that T-pro may represent an expansion within the tumor microenvironment of a preexisting IL17-producing subset of $CD8^+$ T cells that circulates in small quantities in the periphery. According to Kondo *et al*. (2009), IL-17-producing $CD8^+$ T cells are present in small numbers in the peripheral blood of healthy humans, raising the

possibility that such cells can circulate in small numbers in healthy individuals and can expand in certain inflammatory/pathological environments, such as tumors.

T helper 17-differentiated cells have been strongly implicated in the pathogenesis of psoriasis (see Nickoloff *et al*., 2007), which is a cutaneous disorder characterized by neutrophilic and lymphocytic chronic inflammation and epidermal hyperproliferation. Yet, psoriasis has shown little evidence of increased transformation to squamous cell carcinoma within the lesional skin. One possible explanation for this phenomenon is that psoriatic T cells may be further differentiated toward effector TH17, whereas in our system, $CD8^+$ T-pro may resemble regulatory TH17 cells. The latter may produce regulatory factors, such as IL-10, that inhibit cell-mediated immunity (Le Poole *et al*., 2008), which might otherwise help protect against malignant clonal expansion and lower levels of IL-17. Further studies of $CD8^+$ $perforin^{HI}$ versus $CD8^+$ $perforin^{LO}$ populations identified within the infiltrates of human psoriasis lesions and squamous cell carcinoma, and their relationship to $CD8^+$ T-pro observed in our experimental system, may help elucidate the reason why the chronic inflammatory disease psoriasis is apparently resistant to carcinogenesis.

Amphiregulin, one of the several epidermal growth factors (EGFs), has been implicated in stimulating epidermal proliferation in both psoriasis (Cook *et al*., 2004) and squamous cell carcinoma (Billings *et al*., 2003; Berasain *et al*., 2007). The fact that T cells may specifically serve as a major source of amphiregulin production was shown recently in animal models of nematode infections (Zaiss *et al*., 2006). In this model, T-cell secretion of amphiregulin stimulated airway and gut epithelial proliferation that mediated immunoprotection from microbial assault, and in addition also fostered the associated epithelial inflammatory states through previously unrecognized cytokine properties attributable to amphiregulin. It is intriguing to consider that amphiregulin production by $CD8^+$ T-pro might serve a dual role in tumor promotion—through its EGF properties and its inflammation-inducing cytokine activities—that might help link chronic inflammatory states with carcinogenesis (for example, bronchitis, gastritis, colitis with lung, stomach, and colon cancer).

Our findings are consistent with recent studies of anti-IL-17 administration in two-stage chemical carcinogenesis that resulted in decreased DMBA/TPA-induced inflammation, epidermal proliferation, and papilloma formation (Hamada *et al*., 2009; Xiao *et al*., 2009). The information gained by our analyses also suggests how the capacity to pharmacologically target RORγt might be usefully added to the armamentarium of cancer therapy. Nonetheless, a concern for immunotherapy shown in this study is that the “default” situation for T-pro cells in the absence of RORγt may be a T-reg state, as, consistent with other experiments on T-cell differentiation, FoxP3 and IL-10 are enriched in T-pro cells. Although the potent regulatory effects of IL-10 on TH1 cell-mediated immunity have been well established, the role of Tim-3 is more complex. Originally identified as a marker of TH1 differentiation, Tim-3 expression by effector $CD44^{HI}$ $CD62L^{LO}$ CD8+ T cells has recently been reported (Wang *et al*., 2007). Notably, engagement of Tim-3 by its ligand galectin-9 diminished cytotoxicity. Furthermore, Geng *et al*. (2006) recently reported that the soluble form of Tim-3 markedly inhibited T cell-mediated responses and enhanced tumor growth. It is yet to be determined whether $CD8^+$ T-pro facilitate tumor growth by inhibiting antitumor responses by the local production of IL-10 or soluble Tim-3.

Although both $CD4^+$ and $CD8^+$ T-cell responses may be necessary for optimal antitumor immunity (Arbiser *et al*., 2002; Girardi *et al*., 2004), immunotherapy strategies are often designed to stimulate $CD8^+$ T cells in an attempt to produce CTLs capable of tumor-specific cytotoxicity. However, one might consider that within individuals who harbor inflammatory-associated tumors, the possibility exists that the stimulation of $CD8^+$ T cells may enhance the activities of cells with the capacity to facilitate malignant progression. The

experimental system presented provides a pathophysiological context in which to study tumor-promoting T cells by establishing that chemical induction of epithelial tumors results in the infiltration by $CD8^+$ IL-17-producing cells, and that their expression profile is clearly associated with tumor progression. Thus, the analyses presented will help guide further investigation into these potential mechanisms of $CD8^+$ T cell-mediated tumor promotion. In addition, this study may provide insight into inflammatory skin diseases (such as psoriasis) in which there may be mechanistic overlap but seemingly little effect on carcinogenesis (Nickoloff *et al*., 2005).

MATERIALS AND METHODS

Animals and two-stage chemical carcinogenesis

All *in vivo* studies were approved by the Yale Animal Care and Use Committee. FVB/N mice were purchased from Jackson Laboratories (Bar Harbor, ME). $CD4^{-/-}$ and $TCR\beta^{-/-}$ were all backcrossed 15+ generations onto the FVB/N background. The animal facility is Association for Assessment and Accreditation of Laboratory Animal Care accredited. Chemicals were obtained from Sigma (St Louis, MO). DMBA was dissolved in acetone (4mM), and TPA was dissolved in 100% ethanol (0.2mM). Application of DMBA/TPA and tumor monitoring was performed as described previously (Roberts *et al*., 2007). Briefly, initiation by pipette application of 400 (high dose) or 200nmol (low dose) of DMBA was conducted 1 week after shaving back hair using electric clippers, followed by depilatory cream. This was followed by twice weekly application of 20 (high dose) or 5 nmol (low dose) TPA. Cutaneous tumors were counted, measured, and scored weekly as clinically apparent papillomas (typically well-demarcated, symmetrical, pedunculated or dome-shaped papules, without erosion or ulceration), or as clinically apparent carcinomas (poorly demarcated, asymmetrical, non-pedunculated or dome-shaped papules with erosion or ulceration). Tumors were evaluated by visual inspection by an observer (RBF) blinded to the experimental groups. At the conclusion of the experiments, tumors were excised for TIL isolation, or formalin-fixed, paraffin-embedded, and 5-mm-thick sections were hematoxylin and eosin stained and examined (by AG) for histological confirmation.

PBL and TIL isolation

To obtain PBL samples, after anesthesia by methoxyflurane inhalation, mice were individually bled by capillary pipette of the retro-orbital plexus. Approximately 200 μl per mouse was harvested, mixed with 30 μl of heparin 1,000Uml^{-1} (Sigma), and then 5ml D-phosphate-buffered saline. The blood mixture was overlayed on 5ml of Lympholyte-M (Accurate Chemical, Westbury, NY), centrifuged at 600 × *g* for 20 minutes at room temperature, and the interface was harvested and washed twice in Hanks' Balanced Salt solution (HBSS) before overnight incubation in CRPMI (RPMI medium supplemented with 10% FBS, 25mM Hepes, 1mM sodium pyruvate, 100mM nonessential amino acids, 2mM L-glutamine, 2-mercaptoethanol, and antibiotics) at 37 °C in 5% CO_2. To obtain TIL cells, tumors were excised and minced on ice in RPMI 1640 medium supplemented with Hepes pH 7.3, 2-mercaptoethanol, sodium pyruvate, antibiotics, collagenase I (2.5 $mgml^{-1}$) and collagenase II (1.5 $mgml^{-1}$; both from Worthington, Lakewood, NJ), collagenase IV (1 $mgml^{-1}$) and hyaluronidase IV-S (0.25$mgml^{-1}$; both from Sigma), and DNase I (300 gml^{-1}) and soybean trypsin inhibitor (0.06 gml^{-1}; both from Roche, Indianapolis, IN). Suspensions of tumor pieces were incubated at 37 °C for 2 hours. The pieces were then gently pressed between the frosted edges of two sterile glass slides, and cell suspension was passed through sterile 100 μm nylon mesh to remove debris and separate cell aggregates. HBSS (HBSS supplemented with 25mM Hepes, 1mM sodium pyruvate, and antibiotics) was added to stop the digestion. Cells were washed thrice in HBSS before Lympholyte-M gradient separation. TIL were further purified using the gradient as per the manufacturer's protocol, washed

thrice in HBSS and resuspended in CRPMI for overnight incubation at 37 °C in 5% CO_2. The next day, PBL and TIL were washed twice in HBSS and filtered through a 30-μm-thick Nytex filter and stained. Cells were either analyzed by flow cytometry or sorted on a MoFlo (Dako, Glostrup, Denmark) for subsequent expression analysis.

Flow cytometric analysis

Fluorescein isothiocyanate, phycoerythrin, peridinin chlorophyll protein coupled to cyanine dye (PerCP-Cy5.5) or allophycocyanin-conjugated monoclonal antibodies specific for CD3 (145-2C11), CD4 (RM4-5), CD62L (MEL-14), TCRβ (H57-597), CD44 (IM7), IL-17A (TC11-18H10.1) were obtained from BD Biosciences (San Diego, CA), and CD8β (H35-17.2) was from eBioscience (San Diego, CA). For flow cytometry sorting, cells were stained for 30 minutes at 4 °C with a 1:100 dilution for FITC-conjugated antibodies, 1:200 for phycoerythrin conjugated, 1:150 for PerCP-Cy5.5 conjugated, and 1:400 for allophycocyanin conjugated in HBSS, washed twice with HBSS. Intracellular staining for IL-17A was performed using the BD Cytofix/Cytoperm Fixation/Permeabilization Kit (BD Biosciences) according to the manufacturer's protocol. Briefly, sorted cells were incubated in CRPMI with the addition of 50 ng ml^{-1} of phorbol 12-myristate 13-acetate and 1$mgml^{-1}$ of ionomycin (both obtained from Sigma). After 1 hour of incubation, GolgiPlug (Brefeldin A) was added to the media, and cells were harvested for 3 hours and intracellularly stained. Isotype control antibodies were used for background staining. Lymphocyte-gated events were collected on a FACSCalibur and analyzed using CellQuest software (both from Becton Dickenson, San Diego, CA). To view colocalization of IL-17A, TCRβ, and CD8β on TIL, multispectral imaging flow cytometry using ImageStream system and IDEAS3.0 software were used (both from Amnis, Seattle, WA).

Histology

Freshly excised carcinoma tissue was embedded in optical coherence tomography compound and frozen in a bath of 2-methyl-butane chilled on dry ice. Sections of 6-μm thickness were mounted on saline-treated glass slides and purified anti-mouse CD8β (0.5 $mgml^{-1}$; BD Biosciences) was applied. A polyclonal, biotinylated, mouse-anti-rat secondary antibody was followed by strepavidin horseradish peroxidase and the color deposition reaction completed with 3 3′-diaminobenzidine (Dako). Control slides were treated with the biotinylated secondary antibody alone.

RNA isolation and gene-expression analysis

A high-speed, large-scale, flow cytometric sort (MoFlo) was performed on samples from tumor-bearing wt and $CD4^{-/-}$ mice (n = 10–12 each) for $TCR\beta^{+}CD8^{+}CD44^{+}CD62L^{(-)}$ TIL, and compared with parallel sorted PBL cells by expression analysis (>99.5% purity). Total RNA was isolated using RNeasy MicroKit (Qiagen, Valencia, CA) from the purified populations and biotinylated in an amplification protocol using the Illumina TotalPrep RNA Amplification Kit (Ambion, Austin, TX) before hybridization onto Illumina Sentrix Mouse-6 Expression BeadChips (Illumina, San Diego, CA) for comparison of expression levels of 47,000 genes. Illumina probe signal levels were consistent with a purified sorted T-pro population devoid of potentially contaminating CD4+ T cells, NK cells, Langerhans cells, and keratinocytes. Production of differentially expressed genes was confirmed by real-time quantitative reverse transcriptase-PCR (ABI 7500) using SDS 1.4 and SDS 2.0 software (Applied Biosystems, Foster City, CA) on independent isolations from tumor-bearing wt mice. For the latter, RNA was isolated from the sorted population as described earlier and then transcribed using High-Capacity cDNA Reverse Transcription kit (ABI, Foster City, CA). cDNA was amplified using TaqMan PreAmp Master mix and gene specific TaqMan assays (both from ABI) as per the manufacturer's protocol. Preamplified cDNA product was used in downstream TaqMan assays with TaqMan Gene Expression

Master Mix (ABI). Obtained Ct values were normalized against β-actin and expression difference was calculated using the equation $RQ = 2^{-\Delta\Delta Ct}$.

Statistics

Statistical significance was evaluated by the two-tailed, unpaired Student's *t*-test, or nonparametric analysis if SDs were significantly different between the two compared groups. Graphical data are shown with bars indicating SEMs.

Acknowledgments

These studies were supported by N.I.H./N.C.I. grants R01 CA102703 and SPORE P50 CA121974 (MG), the American Skin Association (BK), the Yale Skin Diseases Research Center (N.I.H. P30 AR41942), the Wellcome Trust (TS, ACH), an MRC Programme Grant in psoriasis research (ACH); and were further supported by services provided by the Yale Comprehensive Cancer Center and the Comprehensive Biomedical Research Center. We thank the Dermatology Foundation for career support (MG); the Wellcome Trust Sanger Institute Microarray Facility; Gouzel Tokmoulina for flow cytometry expertise; and Vincent Klump for histopathology expertise.

Abbreviations

CTL	cytolytic T cell
DMBA	7,12-dimethylbenz[*a*]anthracene
Eomes	eomesodermin
HBSS	Hanks' Balanced Salt Solution
PBL	peripheral blood lymphocyte
ROR	retinoic acid–related orphan receptor
TH	T helper
TIL	tumor-infiltrating lymphocyte
TPA	12-*O*-tetradecanoylphorbol 13-acetate
T-pro	tumor-promoting T cells
T-reg	T-regulatory

References

Allavena P, Sica A, Solinas G, et al. The inflammatory microenvironment in tumor progression: the role of tumor-associated macrophages. Crit Rev Oncol Hematol 2008;66:1–9. [PubMed: 17913510]

Arbiser JL, Bingamann A, Durham M, et al. SVR angiosarcomas can be rejected by CD4 costimulation dependent and CD8 costimulation independent pathways. Mol Med 2002;8:551–8. [PubMed: 12456994]

Berasain C, Castillo J, Purgorría MJ, et al. Amphiregulin: a new growth factor in hepatocarcinogeneis. Cancer Lett 2007;254:30–41. [PubMed: 17321672]

Billings SD, Southall MD, Li T, et al. Amphiregulin overexpression results in rapidly growing keratinocytes tumors: an in vivo xenograft model of keratoacanthoma. Am J Pathol 2003;163:2451–8. [PubMed: 14633617]

Cook PW, Brown JR, Cornell KA, et al. Suprabasal expression of human amphiregulin in the epidermis of transgenic mice induces a severe, early-onset, psoriasis-like skin pathology: expression of amphiregul in in the basal epidermis is also associated with synovitis. Exp Dermatol 2004;13:347–56. [PubMed: 15186320]

Coussens LM, Werb Z. Inflammation and cancer. Nature 2002;420:860–7. [PubMed: 12490959]

Finn OJ. Cancer immunology. N Engl J Med 2008;358:2704–15. [PubMed: 18565863]

Galon J, Costes A, Sanchez-Cabo F, et al. Type, density, and location of immune cells within human colorectal tumors predict clinical outcome. Science 2006;313:1960–4. [PubMed: 17008531]

Geng H, Zhang GM, Li D, et al. Soluble form of T cell Ig mucin 3 is an inhibitory molecule in T cell-mediated immune response. J Immunol 2006;176:1411–20. [PubMed: 16424168]

Girardi M, Glusac E, Filler RB, et al. The distinct contributions of murine T cell receptor (TCR)gammadelta+ and TCRalphabeta+ T cells to different stages of chemically induced skin cancer. J Exp Med 2003;5:747–55. [PubMed: 12953094]

Girardi M, Oppenheim D, Glusac EJ, et al. Characterizing the protective component of the alpha/beta T cell response to transplantable squamous cell carcinoma. J Invest Dermatol 2004;122:699–706. [PubMed: 15086556]

Girardi M, Oppenheim DE, Steele CR, et al. Regulation of cutaneous malignancy by gammadelta T cells. Science 2001;294:605–9. [PubMed: 11567106]

Hamada H, Garcia-Hernandez Mde L, Reome JB, et al. Tc17, a unique subset of CD8 T cells that can protect against lethal influenza challenge. J Immunol 2009;182:3469–81. [PubMed: 19265125]

Harris TJ, Grosso JF, Yen HR, et al. Cutting edge: an in vivo requirement for STAT3 signaling in TH17 development and TH17-dependent autoimmunity. J Immunol 2007;179:4313–7. [PubMed: 17878325]

Hennings H, Devor D, Wenk ML, et al. Comparison of two-stage epidermal carcinogenesis initiated by 7,12-imethylbenz(a)anthracene or *N*-methyl-*N*′-nitro-*N*-nitrosoguanidine in newborn and adult SENCAR and BALB/c mice. Cancer Res 1981;41:773–9. [PubMed: 6780187]

Intlekofer AM, Banerjee A, Takemoto N, et al. Anomalous type 17 response to viral infection by $CD8^+$ T cells lacking T-bet and eomesodermin. Science 2008;321:408–11. [PubMed: 18635804]

Koebel CM, Vermi W, Swann JB, et al. Adaptive immunity maintains occult cancer in an equilibrium state. Nature 2007;450:903–7. [PubMed: 18026089]

Kondo T, Takata H, Matsuki F, et al. Cutting edge: phenotypic characterization and differentiation of human CD8+ T cells producing IL-17. J Immunol 2009;182:1794–8. [PubMed: 19201830]

Kryczek I, Bruce AT, Gudjonsson JE, et al. Induction of IL-17+ T cell trafficking and development by IFN-gamma: mechanism and pathological relevance in psoriasis. J Immunol 2006;181:4733–41. [PubMed: 18802076]

Kryczek I, Wei S, Zou L, et al. Cutting edge: Th17 and regulatory T cell dynamics and the regulation by IL-2 in the tumor microenvironment. J Immunol 2007;178:6730–3. [PubMed: 17513719]

Langowski JL, Kastelein RA, Oft M. Swords and plowshares: IL-23 repurposes tumor immune surveillance. Trends Immunol 2007;28:207–12. [PubMed: 17395538]

Langrish CL, Chen Y, Blumenschein WM, et al. IL-23 drives a pathogenic T cell population that induces autoimmune inflammation. J Exp Med 2005;201:233–40. [PubMed: 15657292]

Le Poole C, Denman CJ, Arbiser JL. Immunosuppression may be present within condyloma acuminata. J Am Acad Dermatol 2008;59:967–74. [PubMed: 19022100]

Liu SJ, Tsai JP, Shen CR, et al. Induction of a distinct CD8 Tnc17 subset by transforming growth factor-beta and interleukin-6. J Leukoc Biol 2007;82:354–60. [PubMed: 17505023]

Lochner M, Peduto L, Cherrier M, et al. In vivo equilibrium of proinflammatory IL-17+ and regulatory IL-10+ Foxp3+ RORgammat+ T cells. J Exp Med 2008;205:1381–93. [PubMed: 18504307]

McGeachy MJ, Cua DJ. Th17 cell differentiation: the long and winding road. Immunity 2008;28:445–53. [PubMed: 18400187]

Nam JS, Terabe M, Kang MJ, et al. Transforming growth factor beta subverts the immune system into directly promoting tumor growth through interleukin-17. Cancer Res 2008;68:3915–23. [PubMed: 18483277]

Nickoloff BJ, Ben-Neriah Y, Pikarsky E. Inflammation and cancer: is the link as simple as we think? J Invest Dermatol 2005;124:x–xiv. [PubMed: 15955081]

Nickoloff BJ, Qin JZ, Nestle FO. Immunopathogenesis of psoriasis. Clin Rev Allergy Immunol 2007;33:45–56. [PubMed: 18094946]

Quezada SA, Peggs KS, Simpson TR, et al. Limited tumor infiltration by activated T effector cells restricts the therapeutic activity of regulatory T cell depletion against established melanoma. J Exp Med 2008;205:2125–38. [PubMed: 18725522]

Ribot JC, deBarros A, Pang DJ, et al. CD27 is a thymic determinant of the balance between interferon-gamma- and interleukin 17-producing gammadelta T cell subsets. Nat Immunol 2009;10:427–36. [PubMed: 19270712]

Roberts SJ, Ng BY, Filler RB, et al. Characterizing tumor-promoting T cells in chemically induced cutaneous carcinogenesis. Proc Natl Acad Sci USA 2007;104:6770–5. [PubMed: 17412837]

Sfanos KS, Bruno TC, Maris CH, et al. Phenotypic analysis of prostate-infiltrating lymphocytes reveals TH17 and Treg skewing. Clin Cancer Res 2008;14:3254–61. [PubMed: 18519750]

Strid J, Roberts SJ, Filler RB, et al. Acute upregulation of an NKG2D ligand promotes rapid reorganization of a local immune compartment with pleiotropic effects on carcinogenesis. Nat Immunol 2008;9:146–54. [PubMed: 18176566]

Swann JB, Vesely MD, Silva A, et al. Demonstration of inflammation-induced cancer and cancer immunoediting during primary tumorigenesis. Proc Natl Acad Sci USA 2008;105:652–6. [PubMed: 18178624]

Tomsová M, Melichar B, Sedláková I, et al. Prognostic significance of CD3+ tumor-infiltrating lymphocytes in ovarian carcinoma. Gynecol Oncol 2008;108:415–20. [PubMed: 18037158]

Wang F, He W, Zhou H, et al. The Tim-3 ligand galectin-9 negatively regulates CD8+ alloreactive T cell and prolongs survival of skin graft. Cell Immunol 2007;250:68–74. [PubMed: 18353298]

Wherry EJ, Ha SJ, Kaech SM, et al. Molecular signature of CD8+ T cell exhaustion during chronic viral infection. Immunity 2007;27:670–84. [PubMed: 17950003]

Xiao M, Wang C, Zhang J, et al. IFNgamma promotes papilloma development by up-regulating Th17-associated inflammation. Cancer Res 2009;69:2010–7. [PubMed: 19244111]

Zaiss DM, Yang L, Shah PR, et al. Amphiregulin, a TH2 cytokine enhancing resistance to nematodes. Science 2006;314:1746. [PubMed: 17170297]

Zhang JP, Yan J, Xu J, et al. Increased intratumoral IL-17-producing cells correlate with poor survival in hepatocellular carcinoma patients. J Hepatol 2009;50:980–9. [PubMed: 19329213]

Zhu X, Mulcahy LA, Mohammed RA, et al. IL-17 expression by breast-cancer-associated macrophages: Il-17 promotes invasiveness of breast cancer cell lines. Breast Cancer Res 2008;10:R95. [PubMed: 19014637]

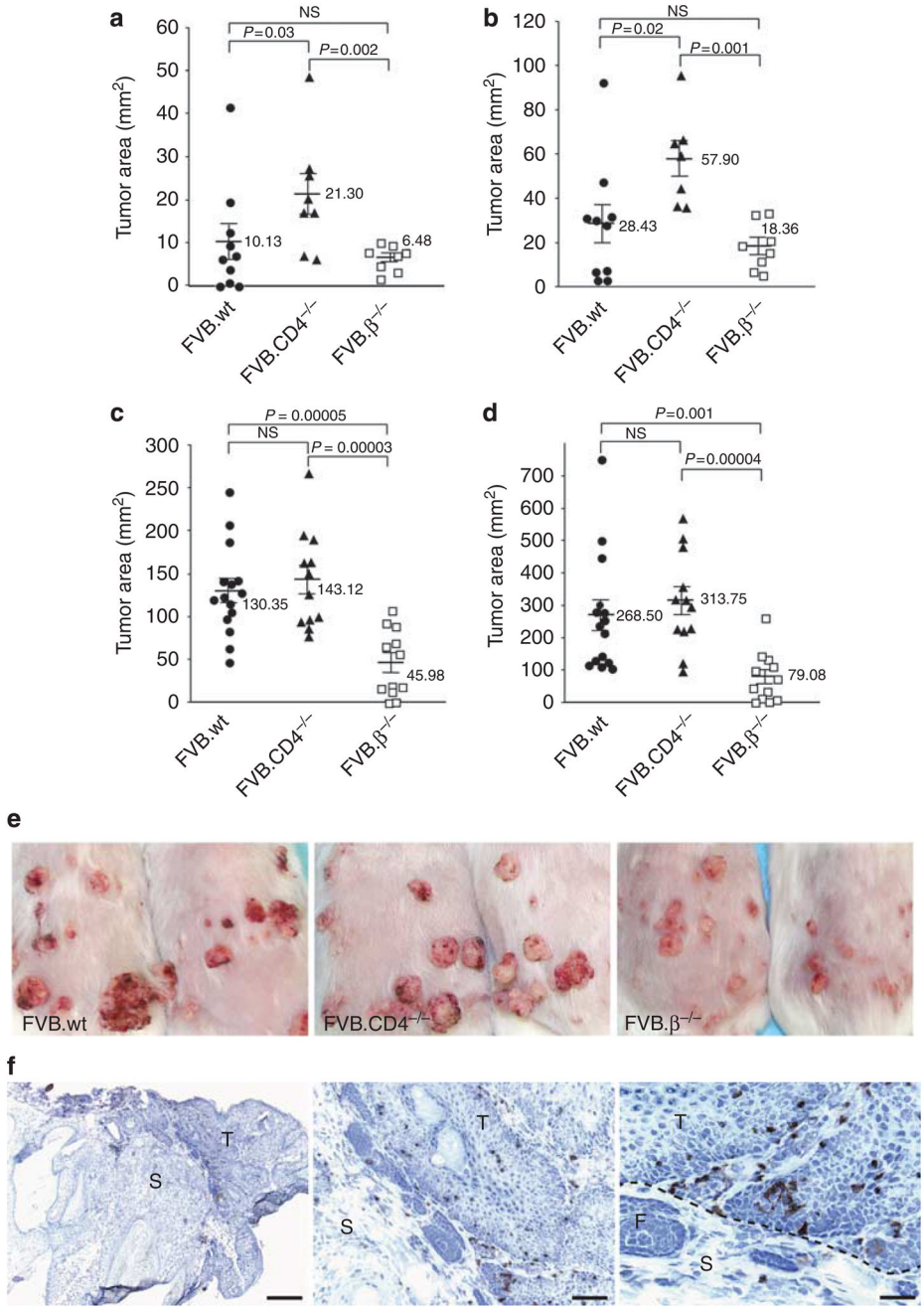

Figure 1. CD8$^+$ T cells infiltrating cutaneous tumors induced by two-stage chemical carcinogenesis are associated with tumor promotion

Tumors were induced on the dorsal skin of FVB wild-type (wt), CD4$^{-/-}$, and TCRβ$^{-/-}$ mice using low-dose (LD) and high-dose (HD) protocols of two-stage chemical carcinogenesis. Under both protocols, augmented tumor susceptibility was greatest in CD8-intact (CD4$^{-/-}$; wt) mice. (**a**, week 12; **b**, week 15): At LD, wt controls produced greater (although not statistically distinguishable) tumor burdens than (TCRβ$^{-/-}$) mice deficient in all TCRαβ$^+$ T cells, whereas CD4$^{-/-}$ mice showed significantly higher tumor susceptibility (P<0.002) than TCRβ$^{-/-}$ mice. (**c**, week 12; **d**, week 15): At HD, tumor burdens were comparably high in both wt and CD4$^{-/-}$ strains compared with TCRβ$^{-/-}$ mice (P<0.001 for wt and P<0.00004

for $CD4^{-/-}$). Error bars, ±SE. (**e**) Tumors that developed under two-stage chemical carcinogenesis were scored as clinically apparent papillomas or carcinomas. Tumor appearance of two representative mice from each of the wt, $CD4^{-/-}$, and $TCR\beta^{-/-}$ cohorts are shown. (**f**) Immunohistochemistry readily identified $CD8^{+}$ cells within tumors (T), but less so in the stroma (S). $CD4^{-/-}$ mouse tumor sections shown; F denotes follicle. Bar = 500, 125, and 60 μm, respectively.

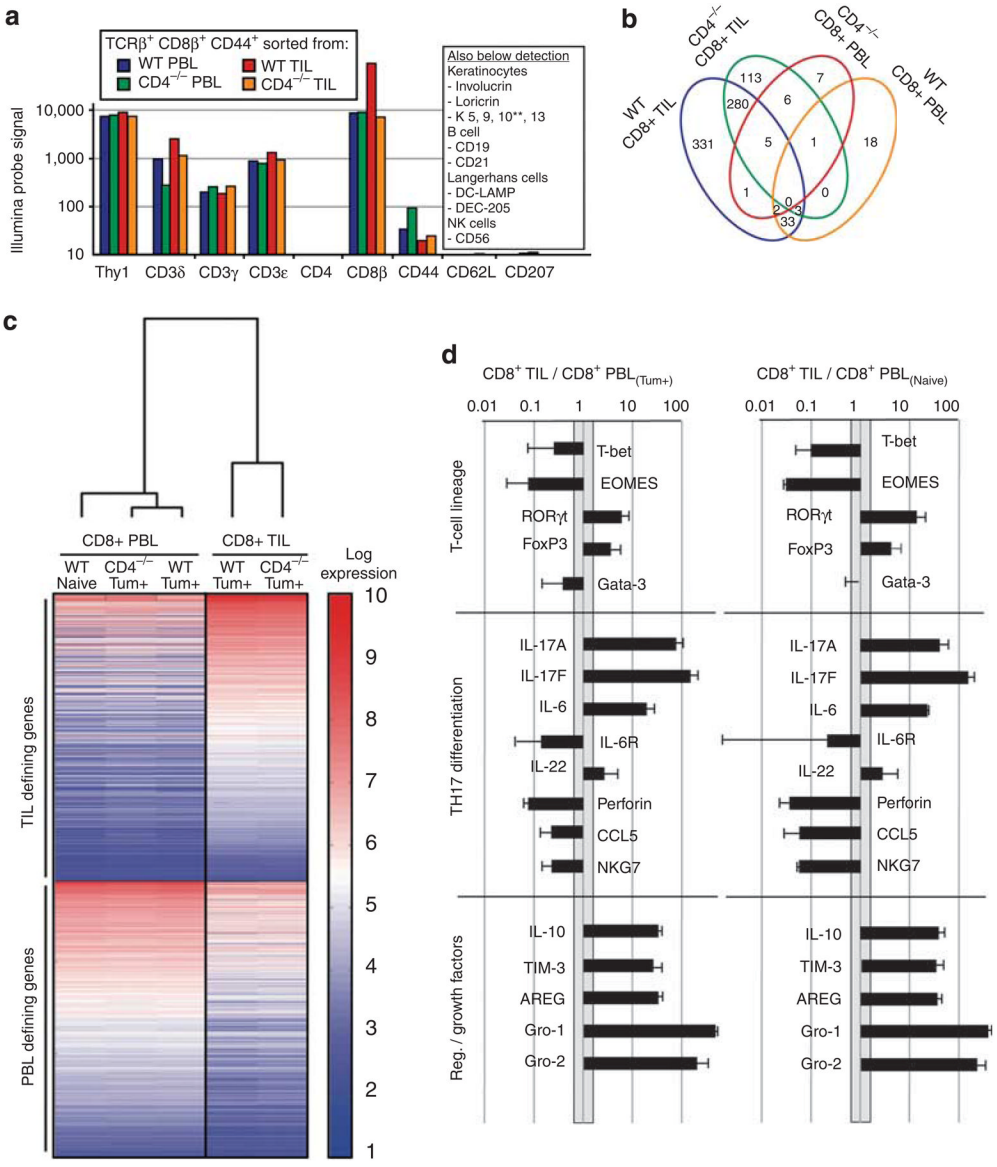

Figure 2. Illumina expression analysis of CD8^{+}TCRβ^{+}CD44^{HI}CD62^{LO} TIL and PBL populations

mRNA from highly purified (>98%) CD44^{HI}CD62L^{LO}TCRβ^{+}CD8^{+} tumor-infiltrating lymphocyte (TIL) and peripheral blood lymphocyte (PBL) from tumor-bearing (Tum^{+}) CD4$^{-/-}$ and Tum^{+} wild-type (wt) mice were analyzed by Illumina Sentrix bead chips (~47,000 genes). (**a**) Absolute probe hybridization values were consistent with high-fidelity purifications. (**b**) Relative to the naive PBL, a total of 800 (~1.7%) genes were found to be >10-fold differentially expressed by the TIL and PBL sorts in Tum^{+} mice. The vast majority of these (91%) were within the TIL sets. (**c**) Hierarchical clustering analysis showed that the PBL populations isolated from tumor-bearing (Tum^{+}) mice were similar to phenotypically equivalent (CD44^{HI}CD62L^{LO}TCRβ^{+}CD8^{+}) effector T cells purified from PBL of naive animals. The dendrogram shows that the primary clusters based on global gene expression differentiate between PBL and TIL, whereas the heatmap (red, high expression; blue, low expression) highlights some of the most differentially expressed genes defining these two major groups. (**d**) Analysis of the most differentially expressed genes unique to CD8^{+} T-pro

(based on absolute probe values) showed differentiation along the RORγt pathway, poor cytotoxic potential, and production of regulatory mediators/growth factors.

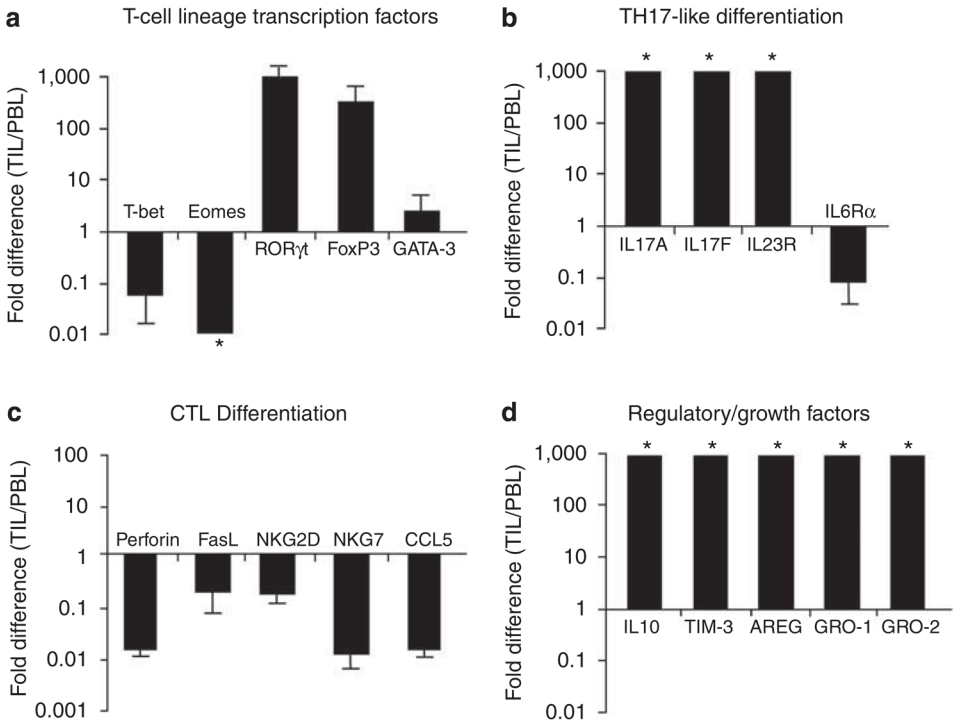

Figure 3. Real-time RT-PCR validation of differentially expressed genes in CD8$^+$ TIL/PBL

Quantitative reverse transcriptase-PCR of mRNA isolated from FVB mouse tumor-infiltrating lymphocyte (TIL) and peripheral blood lymphocyte (PBL) (stained and sorted to >99.5% purity for TCRαβ$^+$CD8$^+$CD44^{HI}CD62L^{LO}) validated key findings from the Illumina expression analysis. Fold-expression differences of TIL/PBL confirmed (**a**, **b**) TH17 differentiation, (**c**) low cytotoxic potential, and (**d**) increased expression of regulatory mediators and growth factors. Error bars, ±SD. Independent isolates (n = 3) for all genes, except Gro-1 and Gro-2 (n = 2). *Ratios beyond designated axes limits.

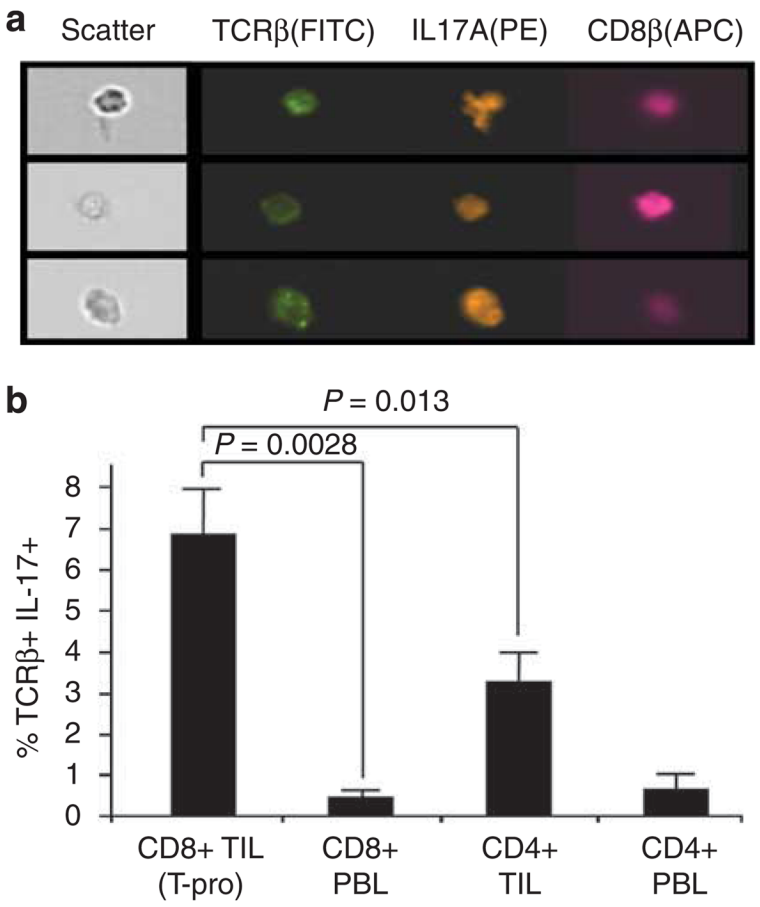

Figure 4. Confirmation of IL-17 production by CD8$^+$ TIL (T-pro)

(**a**) Representative Amnis multispectral imaging identified cells coexpressing TCRβ, IL-17A, and CD8β. (**b**) These analyses showed that IL-17-producing T cells represented a small minority of the CD8$^+$ tumor-infiltrating lymphocyte (TIL) (mean 6.80%; 5 separate isolations).

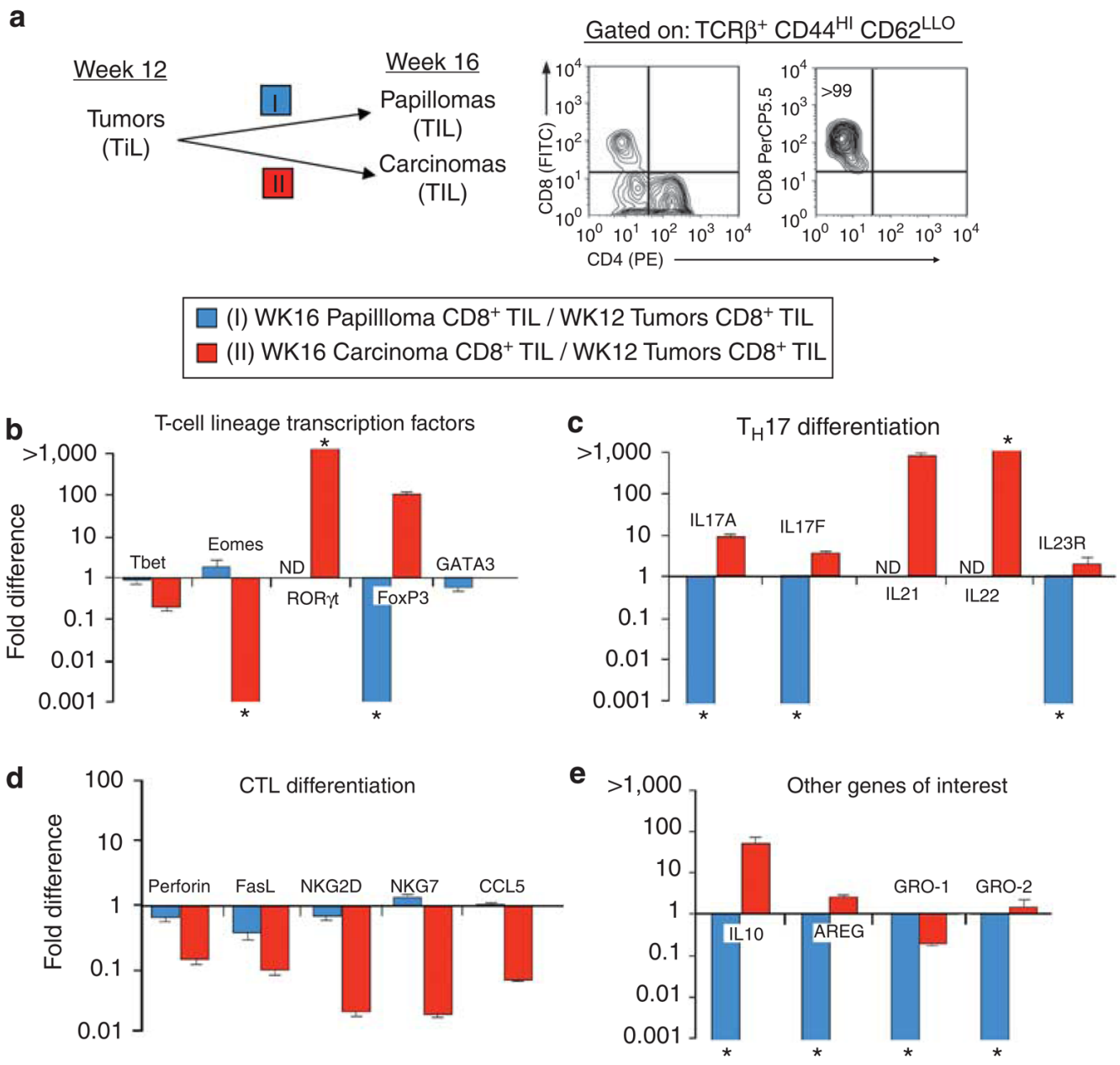

Figure 5. CD8+ T-pro expression profile is associated with malignant progression

(**a**) TIL from week 16 carcinomas (malignant) versus papillomas (benign) were sorted by MoFlo to >99% purity for $CD8^{+}TCR\beta^{+}CD44^{HI}CD62L^{LO}$ and each compared with tumor-infiltrating lymphocyte (TIL) from week 12 aggregate tumors (that is, preponderance of papillomas) by quantitative reverse transcriptase (qRT)-PCR. (**b–e**) The "T-pro profile" was more strongly associated with the CD8+ TIL of malignant tumors (red) than benign tumors (blue) as shown by qRT-PCR. Fold difference of TIL from week 16 carcinomas (malignant) or week 16 papillomas (benign) compared with week 12 aggregate tumors. *n* = 15 mice per group; error bars, SD of triplicate wells; n.d., nondetectable; *Ratios beyond designated axes limits.

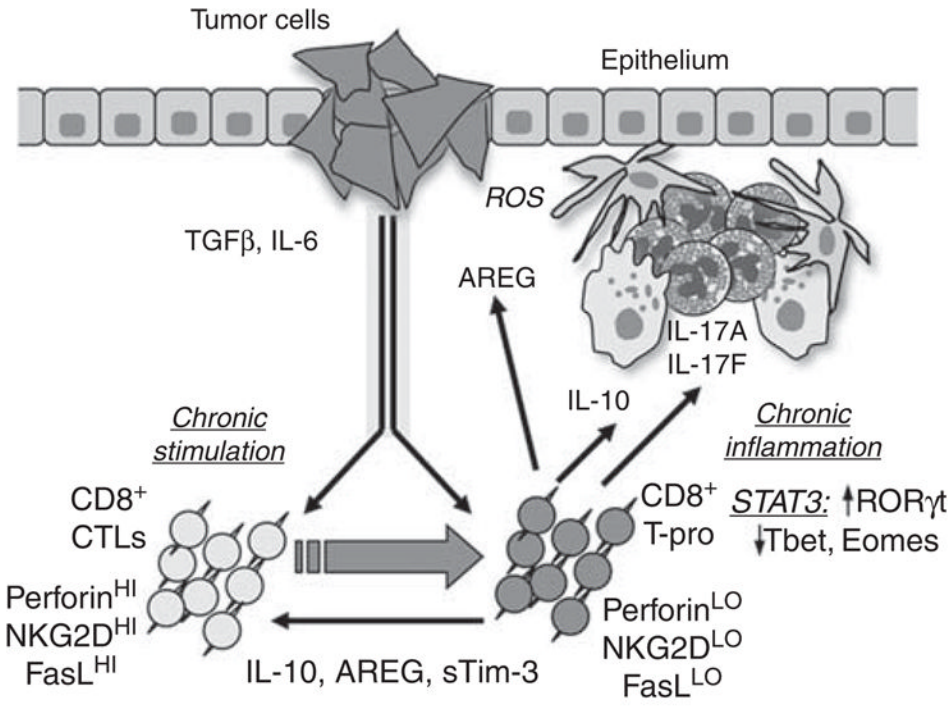

Figure 6. CD8$^+$ T-cell corruption hypothesis

Antitumor CD8$^+$ cytolytic T cells (CTLs) may be redirected into CD8$^+$ T-pro that inhibit T cell-mediated responses (for example, through IL-10), enhance chronic inflammation (for example, through IL-17A and IL-17F), and facilitate tumor proliferation (for example, through AREG and Gro-1).

Table 1

The 30 most differentially upregulated genes in $CD8^+$ TIL (T-pro)

	Gene (aliases)	Name	TIL/PBL fold expression	*P*-value
1	Tff1 (PS2, Bcei)	Trefoil factor 1	628	0.0044
2	Cxcl1 (Gro1, KC, Scyb1)	Chemokine (C-X-C motif) ligand 1	483	0.0002
3	Cxcl2 (Gro2, MIP-2, Scyb2)	Chemokine (C-X-C motif) ligand 2	191	0.0019
4	Ccl17 (TARC, Scya17)	Chemokine (C-C motif) ligand 17	157	0.0006
5	Il17f	Interleukin 17F	153	0.0016
6	Kit (CD117)	C-kit oncogene	95.3	0.0030
7	Scin	Scinderin (adseverin)	87.6	0.0030
8	Il17a (Ctla8)	Interleukin 17A	79.6	0.0043
9	Pdpn (T1a, Gp38, OTS-8)	Podoplanin	72.8	0.0013
10	Anxa3	Annexin A3	64.1	0.0019
11	Tbc1d1	TBC1 domain family, member 1	51.7	0.0008
12	Fam73b	Family with sequence similarity 73, member b	49.3	0.0014
13	Il4i1 (Fig 1)	Interleukin 4 induced 1	48.3	0.0011
14	Basp1 (CAP23)	Brain abundant, membrane attached signal protein 1	45.7	0.0020
15	Mt1	Metallothionein 1	45.4	0.0026
16	Cxcl5 (ENA-78, Scyb5)	Chemokine (C-X-C motif) ligand 5	44.7	0.0041
17	Cdkn1a (P21, CIP1, Waf1)	Cyclin-dependent kinase inhibitor 1A (P21)	44.6	<0.0001
18	Car13	Carbonic anhydrase 13	43.7	0.0045
19	Mmp12 (MMEL)	Matrix metallopeptidase 12	41.7	0.0040
20	Ccl2 (MCP-1)	Ccl2 chemokine (C-C motif) ligand 2	40.9	0.0053
21	Plek2	Pleckstrin 2	40.6	0.0003
22	Lmna	Lamin A/C	39.5	<0.0001
23	Il1b	Interleukin 1 beta	39.4	0.0030
24	Sdc4 (Synd4)	Syndecan 4	39.3	0.0046
25	Clec4n (dectin-2)	C-type lectin domain family 4, member n	36.9	0.0049
26	Areg (Sdgf)	Amphiregulin	34.5	0.0029
27	Slpi	Secretory leukocyte peptidase inhibitor	33.2	0.0030
28	Il10 (CSIF)	Interleukin 10	32.6	0.0018
29	Fam83g	Family with sequence similarity 83, member g	31.3	0.0009
30	Pla1a (Pspla1)	Phospholipase A1 member A	31.1	<0.0001

Abbreviations: PBL, peripheral blood lymphocyte; TIL, tumor-infiltrating lymphocyte.

Table 2

CD8+ T-pro defining genes are associated with progression to carcinoma

WK12 tumors	WK16 papillomas	WK16 carcinomas
Upregulated (TIL/PBL >10)		RORγt
IL-17A		IL-17A
IL-17F		IL-17F
		IL-21
		IL-22
		FoxP3
IL-10		IL-10
Tim-3	Tim-3	Tim-3
AREG		AREG
Gro-1		Gro-1
Gro-2		Gro-2
NKG2D		
Downregulated (TIL/PBL <0.1)		Tbet
		Eomes
Perforin	Perforin	Perforin
		NKG7
		CCL5